ON THE APPLICATION OF TRANSITIONAL FLOW MODELS IN AIRFOIL COMPUTATIONS USING COUPLED NAVIER-STOKES AND e^N TRANSITION PREDICTION METHODS

J.M.M. Sousa
Instituto Superior Tecnico, Mechanical Engineering Dept., 1049-001 Lisboa, Portugal

Abstract

Numerical predictions of the NLF(1)-0416 airfoil operating at moderate Reynolds numbers and low angle of attack have been carried out by coupling Navier-Stokes and e^N *transition prediction methods.*

The consequences of either prescribing point transition or applying a transitional flow model in the Navier-Stokes solver have been systematically investigated. Several classical models have been considered in this study.

1 Introduction

The development of design tools in the framework of laminar flow technology mostly focuses on the generation of reliable transition methods. To this aim, various levels of approach have been considered, ranging from simple empirical relationships to direct numerical simulations. However, for the aircraft industry, the e^N method [1, 2] is the state-of-the-art tool for the prediction of the laminar-turbulent transition onset. The assumptions of local, linear stability and parallel flow are still those most commonly used in this tool [3], though the aforementioned method has already been presented in a multitude of variants. Furthermore, the analysis of three-dimensional flows offers several options for the integration of the N-factor [4], namely the envelope method, the fixed frequency and constant wave propagation direction method, and the fixed frequency and constant total wavelength or constant spanwise wave number methods. Additional options entail the inclusion of compressibility and curvature effects [5]. These variations basically result from the numerous attempts to improve the performance of the e^N method, as it does not account for some fundamental aspects of the transition process. Nevertheless, in nearly 50 years of use, the method has proved its merits and there is still no other practical technique presently available for industrial applications. In addition, the two N-factor method, which enable us handling (in an engineering manner) the simultaneous presence of Tollmien-Schlichting and crossflow instabilities in swept wing flows, has shown great success when applied to wind tunnel and free-flight transonic data [6].

The e^N method is nowadays frequently used in conjunction with viscous-inviscid interaction methodologies for wing design. Recently, the problem of coupling Navier-Stokes codes with the e^N method has also been tackled [7-9]. However, it must be noted at this stage that the modeling of the transition process involves not only the prediction of the transition onset but the prescription of the transition location to the flow solver as well. The latter refers to the coupling procedure between the transition prediction method and flow solver, which encompasses also the application of a transitional flow model. In fact, it has been shown that the foregoing procedure may be of critical importance for the accurate evaluation of aerodynamic performance [8]. Furthermore, the implementation of point transition in Navier-Stokes calculations may, in some cases, prevent iteratively coupled procedures to converge as a result of the upstream influence generated by a too strong viscous-inviscid interaction [8]. Yet, the scatter in predicted transitional lengths hampers the straightforward application of classical transitional flow models.

In this context, the most interesting cases can be found in airfoils operating at moderate Reynolds numbers, for which transition may occur in separated flow regions [7]. As a consequence, the NLF(1)-0416 laminar airfoil [10] operating at Reynolds numbers $Re = 2 \times 10^6$ and 4×10^6 for an angle of attack $\alpha = 1.01°$ has been selected for this investigation. Numerical predictions of the aerodynamic performance of the aforementioned airfoil using coupled Reynolds-averaged Navier-Stokes (RANS) solvers and transition prediction methods have been presented before, e.g. by Krumbein and Stock [11], Stock and Haase [7], Brodeur and van Dam [12] and Stock [8].

The present paper describes a systematic study on the application of classical transitional flow models in RANS computations coupled with the e^N method for transition prediction.

2 Numerical Methods

The RANS solver employed in this investigation is based on a second-order accurate finite volume method. A low-Reynolds number version of the two-equation k-ε turbulence model by Coakley and Huang [13] was used to describe the near-wall region downstream of the transition location. A distinctive characteristic of this version is the fact that its viscosity-related damping functions and some of the numerical constants have been calibrated with reference to data from direct numerical simulations.

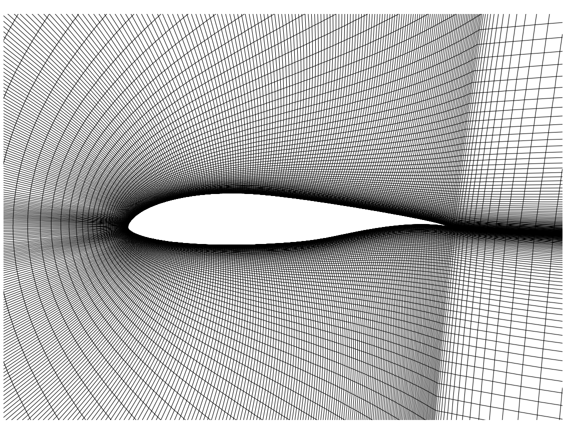

Fig. 1. Airfoil geometry and numerical mesh.

Nonorthogonal, curvilinear meshes formed by 512 x 128 control volumes have been generated through the solution of a system of Poisson equations. Figure 1 shows the airfoil geometry and a partial view of the numerical mesh used.

The e^N method was used for transition prediction based on the linear, local stability analysis of boundary layer profiles [14] produced by the RANS solver.

Additional details concerning the abovementioned methods and the coupling procedure were given by Sousa and Silva [9].

3 Transitional Flow Modeling

The classical approach to transitional flow modeling results from Emmons [15] concept of intermittent appearance of turbulence spots, which grow as they move downstream until they finally merge to form a turbulent boundary layer. Experimental verification of this theory was achieved by Schubauer and Klebanoff [16], Elder [17] and others.

Dhawan and Narasimha [18] have proposed a universal intermittency function, which was adopted in most transitional models. The idea was to define an inttermittency factor (varying from zero to unity) given as the fraction of time occupied by turbulence spots, so that all averaged flow properties of the flow may evolve smoothly from the laminar to the turbulent regime. Although it has been already shown that the intermittency factors vary across the boundary layer both for attached and separated flows [19], it is usually assumed in the classical approaches that wall-normal variations may be neglected. Hence, the intermittency function γ is defined as:

$$\gamma = 1 - \exp\left(-0.412\xi^2\right), \quad (1)$$

where ξ is given by:

$$\xi = \left(X - X_{tr}\right)/\lambda \quad (2)$$

$$X_{tr} = X_{\gamma=0} \quad (3)$$

$$\lambda = X_{\gamma=0.75} - X_{\gamma=0.25}. \quad (4)$$

The downstream limit of the transitional zone, where fully turbulent flow is reached, is defined by:

$$X_{turb} = X_{\gamma=0.99}, \qquad (5)$$

thus yielding the following expression for the transition length:

$$L_{tr} = X_{turb} - X_{tr} = 3.36\lambda \, . \qquad (6)$$

Examples of classical models for the transition length L_{tr}, corresponding to incompressible flat plate flows are:

- Narasimha model [20]

$$Re_{L_{tr}} = 30.2 Re_{X_{tr}}^{3/4}, \qquad (7)$$

- Chen and Thyson model [21]

$$Re_{L_{tr}} = 60 Re_{X_{tr}}^{2/3}, \qquad (8)$$

- Walker model [22]

$$Re_{L_{tr}} = 5.2 Re_{X_{tr}}^{3/4}. \qquad (9)$$

It can be easily concluded that these models produce a wide range of possible values for the transition length. For example, a direct comparison between Eqs. (7) and (9) indicates nearly a six-fold variation in L_{tr} for the same value of the local Reynolds number. As an attempt to reduce this scatter and to cope with pressure gradient flows, it was suggested that boundary layer history effects should be introduced in the models, thus replacing the X-coordinate at transition by an appropriate boundary layer property. Stock and Haase [7] have proposed the use of the displacement thickness as scaling property, resorting to the incompressible flat plate Blasius flow relation. Hence, modified versions of the models above may be derived as follows:

- Narasimha model (modified)

$$Re_{L_{tr}} = 13.4 Re_{\delta_{tr}^*}^{3/2}, \qquad (10)$$

- Chen and Thyson model (modified)

$$Re_{L_{tr}} = 29.1 Re_{\delta_{tr}^*}^{4/3}, \qquad (11)$$

- Walker model (modified)

$$Re_{L_{tr}} = 2.3 Re_{\delta_{tr}^*}^{3/2}. \qquad (12)$$

Measurements by Gostelow, Blunden and Walker [23] have shown a strong dependency of the transition length with the pressure gradient. However, the use of a Blasius flow relation to account for this effect seems rather inconsistent. A sensible alternative procedure may be the application of Cebeci and Smith [24] version of Chen and Thyson model [21], which assumes that spot propagation velocities at any given X-location are proportional to the local external velocity $U_e(X)$, thus yielding the following expression for the intermittency factor:

$$\gamma = 1 - \exp\left[-G(X - X_{tr}) \int_{X_{tr}}^{X} \left(\frac{dX}{U_e} \right) \right], \qquad (13)$$

where G stands for a spot formation rate parameter given by:

$$G = (1/1200)\left(U_e^3/\nu^2\right) Re_{tr}^{-1.34} \, . \qquad (14)$$

As pointed out by Walker [25], an additional though more complex option consists in the recent innovation of using intermittency transport models to compute the variation of the turbulent intermittency through the transition zone. This procedure is currently under investigation following the suggestions of Suzen and Huang [26]. They have shown its viability using Menter's SST model [27] for flows with and without pressure gradient, in the presence of significant free-stream turbulence effects. It was observed that consistent intermittency factor profiles might be obtained. Furthermore, these differed significantly from the simple empirical formula proposed by Klebanoff [28] to describe the cross-stream variation of intermittency in a turbulent boundary layer.

4 Results and Discussion

Initial computations of the NLF(1)-0416 airfoil have been carried out at Reynolds numbers Re = 2 x 10^6 and 4 x 10^6 for an angle of attack α = 1.01° prescribing point transition in the

RANS solver. The pressure distribution resulting from the application of coupled RANS and e^N methods to these cases is shown in Fig. 2. Very good agreement can be observed between the numerical predictions at Re = 4 x 10^6 and the experimental data (symbols, [10]). The small differences between the numerical results obtained for the different values of the reference Reynolds number are mainly a consequence of the distinct transition locations.

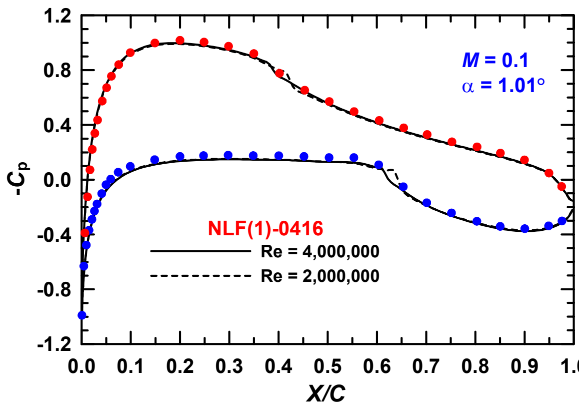

Fig. 2. Numerical predictions of the pressure distribution using point transition (symbols denote experiments).

Excellent agreement between computed and experimental transition locations [10] was obtained, irrespective of the fact that point transition has been used. These results are illustrated in Fig. 3 for a limiting N-factor of 11, which is the same value used in previous studies of the present airfoil (Note: the light blue bands indicate experimental transition data).

a)

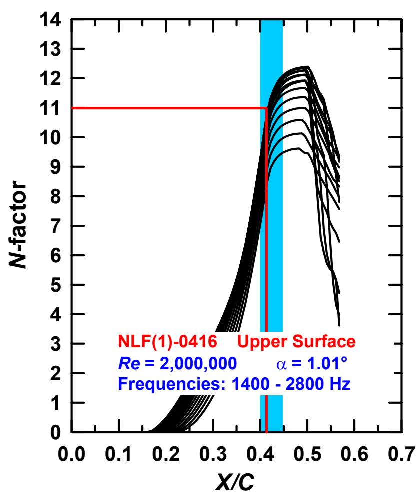

b)

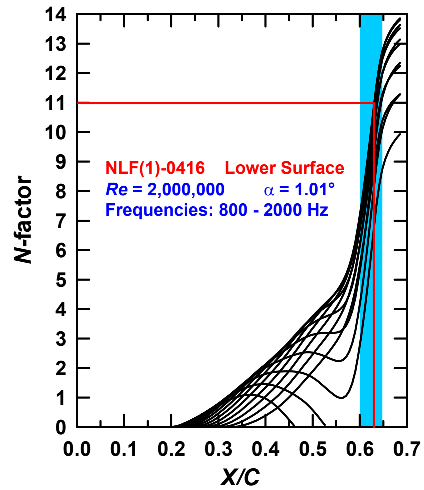

Fig. 3. Predicted transition locations using point transition for $Re = 2 \times 10^6$:
a) upper surface;
b) lower surface.

Figure 4 shows the computed evolutions of the skin friction coefficient for both computations. The results indicate that a small separation bubble is formed both on upper and lower surfaces of the airfoil for Re = 2 x 10^6. However, the flow does not separate on the upper surface for Re = 4 x 10^6, which is again in agreement with experimental observations [10]. An additional computation has been carried out for the lower value of the Reynolds number by prescribing the transition locations at laminar separation on both surfaces (obtained from the previous point transition computation).

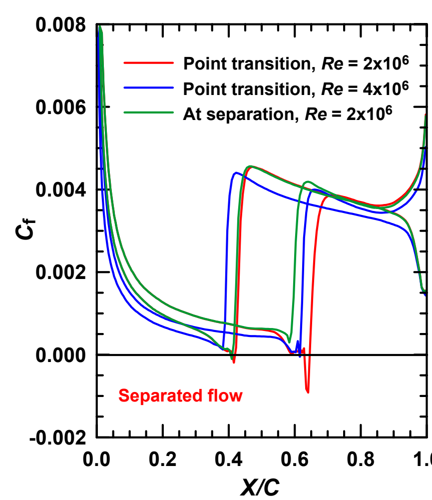

Fig. 4. Evolution of the skin friction coefficient using point transition.

Based on these preliminary computations, it was possible to perform the *a priori* investigation of the performance of the various transitional flow models. Figure 5 portrays the evolution of L_{tr} as a function of the transition location for $Re = 4 \times 10^6$. It must be noted that the results for $Re = 2 \times 10^6$ show similar trends but the values of L_{tr} are even higher. The figure indicates that the modified versions of the models (dotted lines) generate very large transition lengths in the presence of a separation bubble, as a consequence of the sharp increase in displacement thickness. This does not seem to be physically correct, as the transition is expected to be rapid (though not a point phenomenon) in separated flow. In addition, it can be easily concluded that the model of Narasimha ([20], modified or not) is clearly inadequate for this type of flows, producing transition lengths which extend up to the airfoil trailing edge and beyond.

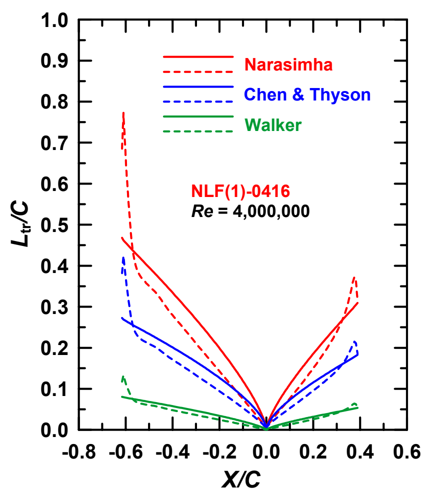

Fig. 5. *A priori* evaluation of the transition length generated by the various models at $Re = 4 \times 10^6$.

New computations using the coupled methods have been carried out for both values of the Reynolds number employing transitional models instead. Results have been obtained (when possible) for the base and modified versions of the model of Walker [22]. In addition the application of Chen and Thyson model has also been investigated. However, preference was given to the implementation used by Cebeci and Smith [24], as described by Eqs. (13)-(14).

All transitional flow models led to a very slight upstream movement of the predicted transition location (maximum: $0.01C$). This result can be appreciated in Fig. 6 for $Re = 2 \times 10^6$ as an example.

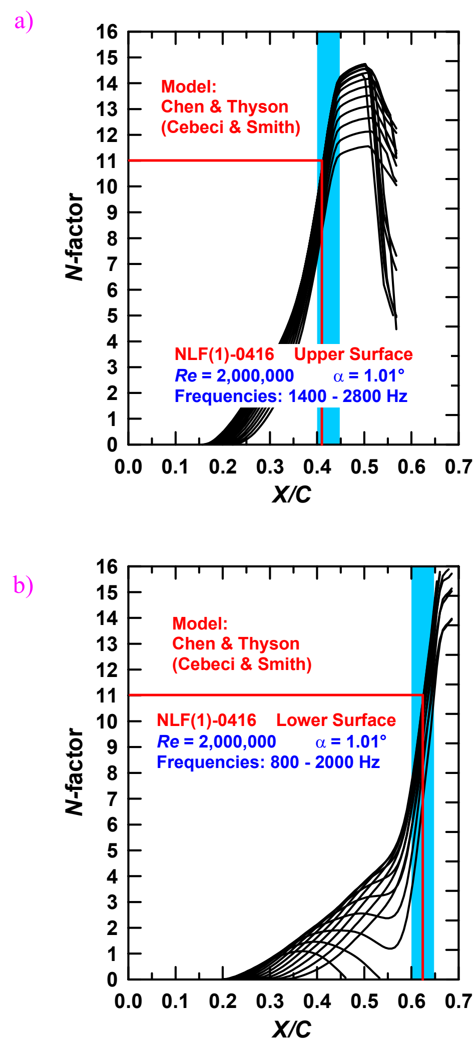

Fig. 6. Predicted transition locations using Cebeci and Smith version of Chen and Thyson transitional model for $Re = 2 \times 10^6$:
a) upper surface;
b) lower surface.

The use of transitional models has improved the convergence between the coupled methods in order to reach a common transition location (within $0.005C$). However, due to the establishment of larger separation bubbles, a larger number of iterations was required to obtain a solution from the RANS solver.

A summary of the transition locations produced by the coupled methods and the transitional lengths obtained for all solutions is provided in Table 1. The serial number of the numerical simulation is also identified in this table for later reference in the paper.

Table 1. Predicted transition locations and transition lengths for all computations.

N	Model, Reynolds No.	$(X/C)_{tr}$		L_{tr}/C	
		upper	lower	upper	lower
1	Point, 2x10^6	0.42	0.63	–	–
2	Point, 4x10^6	0.385	0.61	–	–
3	Separation, 2x10^6	0.41	0.59	–	–
4	Walker, 2x10^6	0.41	0.625	0.066	0.072
5	Walker, 4x10^6	0.38	0.605	0.052	0.057
6	Walker modif, 2x10^6	–	–	0.115	0.347
7	Walker modif, 4x10^6	0.38	0.605	0.066	0.136
8	Chen/Thyson, 2x10^6	0.41	0.625	0.119	0.158
9	Chen/Thyson, 4x10^6	0.38	0.605	0.100	0.131

As an example, the evolution of the skin friction coefficient using the transitional models is presented in Fig. 7 for $Re = 4 \times 10^6$. Similar trends were obtained for $Re = 2 \times 10^6$, though flow separation occurs on both sides of the airfoil and a stable converged solution could not be obtained for the modified version of the model of Walker [22] due to the large value of L_{tr} obtained for the lower surface (Cf. Table 1). It is interesting to note that Krumbein [29] has also reported convergence problems with the use of this model on a high-lift multi-element airfoil configuration.

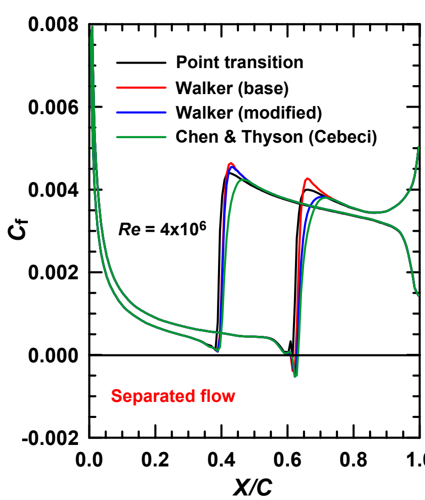

Fig. 7. Evolution of the skin friction coefficient using transitional flow models for $Re = 4 \times 10^6$.

The transitional models provide a smoother transition in C_f than point transition. However, small values of L_{tr} produce locally high values of C_f in the turbulent regime.

In order to investigate the consequences of using transitional flow models in the analysis of the aerodynamic performance of the airfoil, the values of lift and drag coefficients have been evaluated. The results have been summarized in Table 2.

Table 2. Predicted aerodynamic coefficients for all computations (experimental data is also given).

N	Numerical predictions			Experiments	
	C_L	$C_{D\text{-}surf}$	$C_{D\text{-}wip}$	C_L	C_D
1	0.575	0.0082	0.0069	0.550	0.0071
2	0.584	0.0075	0.0062	0.561	0.0059
3	0.575	0.0084	0.0070	0.550	0.0071
4	0.576	0.0083	0.0068	0.550	0.0071
5	0.585	0.0075	0.0061	0.561	0.0059
6	–	–	–	0.550	0.0071
7	0.585	0.0075	0.0060	0.561	0.0059
8	0.576	0.0081	0.0068	0.550	0.0071
9	0.585	0.0073	0.0060	0.561	0.0059

The values of the drag coefficient obtained by surface integration $C_{D\text{-}surf}$ have shown always to overpredict the experimental values. However, the application of the transitional flow models has, in some cases, brought these two values closer to each other. Excellent results were always obtained when the drag coefficient was evaluated through a wake integration procedure $C_{D\text{-}wip}$ [30]. Furthermore, it observed that the coupled methods systematically overpredict the experimental values of the lift coefficient C_L. However, this is in agreement with previous studies of the present airfoil and it was argued that this anomaly might be due to uncorrected wind-tunnel effects [8].

5 Conclusions

The coupled RANS/e^N computations carried out for the NLF(1)-0416 airfoil at moderate Reynolds numbers and low angle of attack have shown that the use of transitional flow models is recommended though not indispensable. In addition, care should be taken when these are applied because the classical models often produce disparate values of the transitional length, especially in the presence of separated flow. Such behavior may ultimately preclude the generation of converged solutions by the RANS solver.

References

[1] van Ingen JL. A suggested semi-empirical method for the calculation of the boundary layer transition region. Dept. of Aerospace Engineering, Report VTH-74, University of Delft, The Netherlands, 1956.

[2] Smith AMO and Gamberoni N. Transition, pressure gradient and stability theory. Douglas Aircraft Co., Report ES 26388, Long Beach, California, 1956.

[3] Joslin RD. Overview of laminar flow control. NASA TP 1998-208705, Langley Research Center, Hampton, Virginia, 1998.

[4] Malik MR and Orszag SA. Comparison of methods for prediction of transition by stability analysis. *AIAA Journal*, Vol. 18, No. 12, pp 1485-1489, 1980.

[5] Pereira JCF and Sousa JMM. Comparison of several *N*-factor integration strategies in a compressible boundary layer over a swept curved surface. *Proc 19th Congress of the International Council of the Aeronautical Sciences*, Anaheim, California, Vol. 2, ICAS paper 94-2.4.2, pp 1093-1103, 1994.

[6] Schrauf G. Large-scale laminar flow tests evaluated with linear stability theory. AIAA paper 2001-2444, 2001.

[7] Stock HW and Haase W. Navier-Stokes airfoil computations with e^N transition prediction including transitional flow regions. *AIAA Journal*, Vol. 38, No. 11, pp 2059-2066, 2000.

[8] Stock HW. Airfoil validation using coupled Navier-Stokes and e^N transition prediction methods. *AIAA Journal*, Vol. 39, No. 1, pp 51-58, 2002.

[9] Sousa JMM and Silva LMG. Transition prediction in infinite swept wings using Navier-Stokes computations and linear stability theory. *Computers and Structures*, 2004 (in press).

[10] Somers DM. Design and experimental results for a natural-laminar-flow airfoil for general aviation applications. NASA TP 1861, Langley Research Center, Hampton, Virginia, 1981.

[11] Krumbein A and Stock HW. Laminar-turbulent transition modelling in Navier-Stokes flow solvers using engineering methods. *Proc European Congress on Computational Methods in Applied Sciences and Engineering*, Barcelona, Spain, 2000.

[12] Brodeur RR and van Dam CP. Transition prediction for a two-dimensional Reynolds-averaged Navier-Stokes method applied to wind turbine airfoils. *Wind Energy*, Vol. 4, pp 61-75, 2001.

[13] Coakley TJ and Huang PG. Turbulence modelling for high-speed flows. AIAA paper 92-0436, 1992.

[14] Mack LM. Boundary-layer linear stability theory. Special course on stability and transition of laminar flows. AGARD Report 709, 1984.

[15] Emmons HW. The laminar-turbulent transition in a boundary layer – Part I. *Journal of the Aerospace Sciences*, Vol. 18, No. 7, pp 490-498, 1951.

[16] Schubauer GB and Klebanoff PS. Contributions on the mechanics of boundary layer transition. NACA Report 1289, 1955.

[17] Elder J. An experimental investigation of turbulent spots and breakdown to turbulence. *Journal of Fluid Mechanics*, Vol. 9, pp 235-246, 1960.

[18] Dhawan S and Narasimha R. Some properties of boundary layer flow during transition from laminar to turbulent motion. *Journal of Fluid Mechanics*, Vol. 3, pp 418-436, 1958.

[19] Hazarika BK and Hirsch C. Intermittency distribution in attached and separated boundary layers. *ERCOFTAC Bulletin*, Vol. 24, pp 17-20, 1995.

[20] Narasimha R. A note on certain turbulent spot and burst frequencies. Dept. of Aeronautical Engineering, Report 78 FM 10, Indian Institute of Science, Bangalore, India, 1978.

[21] Chen KK and Thyson NA. Extension of Emmon's spot theory to flows on blunt bodies. *AIAA Journal*, Vol. 9, No. 5, pp 821-825, 1971.

[22] Walker GJ. Transitional flow on axial turbomachine blading. *AIAA Journal*, Vol. 27, No. 5, pp 595-602, 1989.

[23] Gostelow JP, Blunden AR and Walker GJ. Effects of free-stream turbulence and adverse pressure gradients on boundary layer transition. *ASME Journal of Turbomachinery*, Vol. 116, No. 7, pp 392-404, 1994.

[24] Cebeci T and Smith AMO. *Analysis of turbulent boundary layers*. Academic Press, New York, 1974.

[25] Walker GJ. Laminar-turbulent transition in airfoil flows. *Proc Simposium on Advances in Fluid Mechanics*, pp 234-245, 2003.

[26] Suzen YB and Huang PG. Modelling of flow transition using an intermittency transport equation. *ASME Journal of Fluids Engineering*, Vol. 122, No. 2, pp 273-284, 2000.

[27] Menter FR. Two-equation eddy-viscosity turbulence models for engineering applications. *AIAA Journal*, Vol. 32, No. 8, pp 1598-1605, 1994.

[28] Klebanoff PS. Characteristics of turbulence in a boundary layer with zero pressure gradient. NACA Report 1247, 1955.

[29] Krumbein A. On modeling of transitional flow and its application on a high lift multi-element airfoil configuration. *Proc 41st Aerospace Sciences Meeting and Exhibit*, Reno, Nevada, AIAA paper 2003-724, 2003.

[30] Janus JM and Chatterjee A. Use of a wake-integral method for computational drag analysis. *AIAA Journal*, Vol. 34, No. 1, pp 188-190, 1996.